Structure and stability of the plasma crystal

A. Melzer, V. A. Schweigert,* I. V. Schweigert,† A. Homann, S. Peters, and A. Piel
Institut für Experimentalphysik, Christian-Albrechts-Universität Kiel, 24098 Kiel, Germany
(Received 17 November 1995)

The plasma crystal formed by monodisperse particles trapped in the sheath of an rf discharge is known to show vertically aligned structures. Here, oscillations of the aligned particles are found below a threshold value of gas density as a precursor of the melting transition. Attractive forces due to the formation of a positive space-charge region below the upper particle are calculated from Monte Carlo simulations of ion trajectories in the sheath. The alignment as well as the oscillations of the plasma crystal are explained by a simple model based on the asymmetry of the forces. [S1063-651X(96)50307-7]

PACS number(s): 52.25.Vy, 52.35.−g, 62.30.+d

The formation of Wigner crystals in dusty plasmas has attracted much interest very recently. Dust particles immersed in a plasma interact by means of the Coulomb repulsion of the particle's charges acquired by electron and ion currents. Ikezi [1] theoretically predicted plasma conditions under which these particles should form regular lattices, the so-called plasma crystal. Experimentally these crystals were found by Chu and co-workers [2–4] in a magnetron rf discharge with trapped discharge-grown SiO_2 particles. Thomas *et al.* [5] and Melzer *et al.* [6,7] found plasma crystals in parallel plate rf discharges where dust particles intentionally added to the plasma are trapped in the sheath of the lower electrode, where mainly the upward-directed field force balances the gravitational force on the particles. The dust grains arrange in a flat crystal with a diameter of a few hundred interparticle distances and a thickness of up to 20 layers, with usual two-dimensional (2D) hexagonal order in the plane. In the vertical direction the particles are found to be aligned [4,7,8].

In this paper we show that the alignment can be explained by nonreciprocal attractive forces on the particles due to ion streaming motion. These forces overcome the dust Coulomb repulsion. They are also responsible for the onset of particle oscillations about the aligned positions, which are compared with experimental findings.

The measurements were performed in a parallel plate rf discharge at 13.56 MHz and a power input of 12 W with the lower electrode powered and the upper grounded. The discharge was operated in helium at pressures ranging from 30 to 150 Pa. Monodisperse spherical melamine/formaldehyde particles of 4.8 μm and 9.4 μm diameter were added to the plasma. The choice of different particle sizes provides a change of the gravitational force by a factor of about 8. The dust crystal is illuminated by a vertical or horizontal laser fan and is observed in scattered light with a video camera. The experimental setup has been decribed in detail in [7]. The charge on the dust particles is determined from the resonance frequency in the potential well formed by the gravitational and electrical forces [6–8]. The measured charge is $Z_- = 15\,000$ elementary charges corresponding to a surface potential of $\phi = -5$ V for the 9.4-μm particles ($Z_- = 3600, \phi = -2.2$ V for the 4.8-μm particles). Figure 1 shows a side view of the crystal formed by the larger particles at a pressure of 118 Pa. One can see that the dust crystal consists of two aligned layers in contrast to a close-packed structure, which is a minimum energy state for repulsive forces. The possibility of attractive forces by polarization of the ion flow were recently discussed in [9,10]. bcc and fcc structures [4] were reported for laterally constricted systems, but in our experiment the aligned particle arrangement is always found for both particle sizes. With an increasing number of layers the particles still form vertically aligned chains. We restrict further discussion to the case of two layers in order to compare with a simple model. The interparticle distance is $a = 450$ μm in the horizontal direction and $d = 360$ μm in the vertical direction for the larger particles ($a = 350$ μm, $d = 280$ μm for the smaller grains).

Another important feature of this particle arrangement is revealed when the gas density is reduced. Then the particles start to oscillate horizontally about their equilibrium positions (see Fig. 2) at a frequency in the range of 8 to 20 Hz with amplitudes of some 10 μm. The amplitudes of the lower-layer particles are greater by about a factor of 2 than that of the upper-layer particles. The upper particles have a phase lead of about $50° \pm 30°$. The peculiarity lies in the fact that these oscillations have a sharp onset when the gas density is reduced and that the density is so high that all externally forced oscillations are still damped out within milliseconds. Furthermore, these oscillations seem to be a precursor for the phase transition from solid to liquid when the gas density is reduced [8].

We have carried out extensive Monte Carlo (MC) simu-

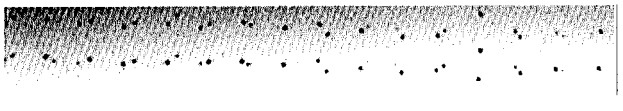

FIG. 1. Inverted video image of the plasma crystal—side view.

*Permanent address: Institute of Theoretical and Applied Mechanics, 630090 Novosibirsk, Russia.

†Permanent address: Institute of Semiconductor Physics, 630090 Novosibirsk, Russia.

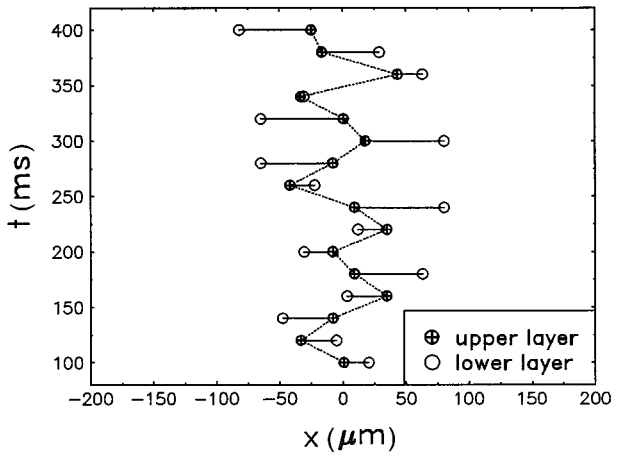

FIG. 2. Horizontal oscillations of upper and lower particles.

lations to determine the forces by distortion of the ion trajectories in the sheath.

The system studied consists of two hexagonal layers of dust particles with the interparticle and vertical distances taken from the experiment ($a=450$ μm, $d=360$ μm). The particle potential was fixed at $\phi=-5$ V. In the experiment the crystal is suspended in the sheath above the lower electrode by a nearly linearly increasing electric field [11]. Therefore, such an electric field is superimposed on the Coulomb field of the dust grains in the simulation. Charge-exchange collisions are also taken into account. From the ion trajectories the forces acting on the dust particles are calculated.

Figure 3 shows a contour plot of the ion density (averaged over angle) from the MC simulation with an ion mean-free path of 100 μm, which corresponds to a pressure of about 100 Pa. The dust particles are vertically aligned and are located at $r=0$ μm and $z=0$ μm (upper) and $z=360$ μm (lower), where r,z denote cylindrical coordinates. In the radial direction only half the spacing to the next neighbor at $r=450$ μm is shown. One can identify three different regions in this plot. For $r>100$ μm there is an almost undisturbed region (region 3). Here the ion density slowly decreases with increasing z because of the ion acceleration by the electric field. Close to the dust particles (region 1) there is a very high ion density due to trapped ions in the potential well of the dust particles. Below the dust particles one can see a region (region 2) of enhanced ion density (ion cloud) with respect to the undisturbed ion density. It is formed by ions which are deflected by the attractive forces between dust particles and ions. The ion cloud of the *upper* particle provides an attractive force for the *lower* dust particles. This is the reason for the alignment of the particles. A similar focusing effect was found in collisionless models of the ion flow around dust grains [9,10]. Our approach, however, is more realistic in that it includes ion acceleration in the sheath and charge-exchange collisions, which counteract the focusing.

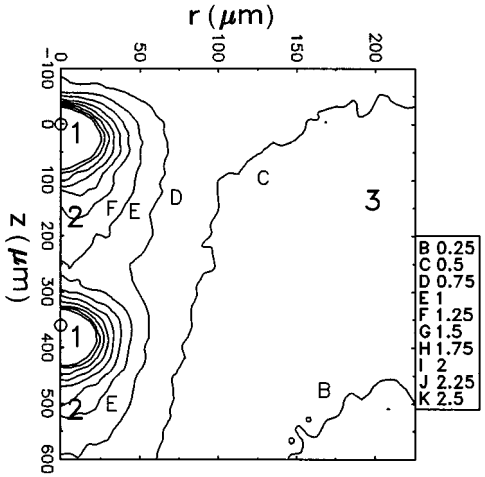

FIG. 3. Ion density distribution obtained from Monte Carlo simulations. The ion density is given relative to the density at the simulation boundary at $z=-500$ μm.

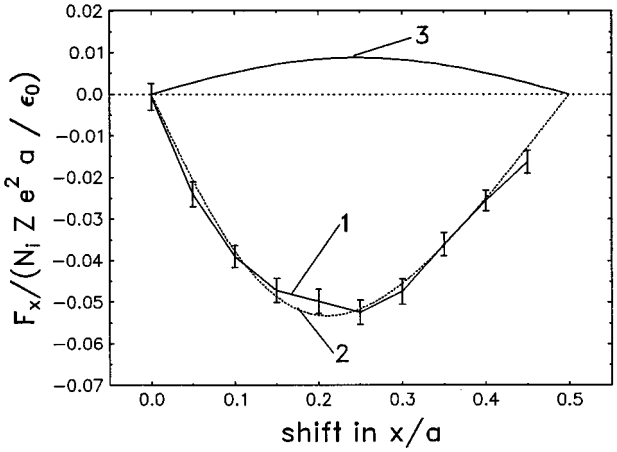

FIG. 4. Forces acting on the lower particle when the lower layer is shifted as a whole with respect to the upper layer. (1) Attractive force resulting from MC simulation; (2) attractive force obtained from the model system with $\gamma=0.5$ and $\delta=0.4$; (3) repulsive force of the upper layer.

When the lower dust layer as a whole is shifted with respect to the upper layer, then the ion cloud is still found directly below the *upper* particle and is only slightly affected by the position of the *lower* particle layer. On the other hand, there is a strong restoring force on the lower particle provided by the ion cloud. These findings are the key points in the further discussion of the stability of this dust particle arrangement.

In Fig. 4 the horizontal component of the forces on the lower particle are compiled when the lower layer is shifted with respect to the upper layer. The repulsive force between the particles of the lower and upper layers is given as curve 3. Curve 1 shows the attractive force by the ion cloud. This force is negative because it is restoring. It is important to emphasize here that an equivalent attractive force for the *upper* particle does not exist, because the ion cloud is created by the upper particle and is always located below it. Hence the vertical alignment is explained by the horizontally attractive force on the lower particle due to an accumulation of ions behind the upper particle. This attractive force outweighs the repulsive forces between the dust particles.

The stability of this particle arrangement and the oscilla-

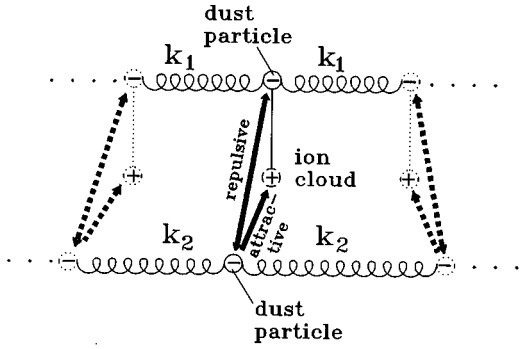

FIG. 5. The coupled chain model.

tions of the particles about their aligned positions can be studied analytically in a model which is derived from the MC results. The ion cloud below the upper particle is in our model represented by a massless positive point charge Z_i at a vertical distance $d-d_i$ below the upper particle. The values of $\gamma=Z_i/Z_-$ and $\delta=d_i/d$ are chosen in such a way that their attractive force on the lower particle fits the MC results (see Fig. 4, curve 2). The positive charge is treated as being rigidly attached to the upper particle as seen in the MC simulations. On the particles of the lower layer act the attractive forces of the positive point charges and the repulsive forces of the upper particles, whereas on the upper particles act only repulsive forces from the lower layer. There is no attractive force for the upper particles, and also the positive charge is not attracted by the lower layer, as found from the MC simulations. Hence there is an asymmetry in the forces between the upper and the lower particles. It is this asymmetry which determines the stability and oscillations of the crystal.

The linear stability analysis for the full model with two hexagonal layers, taking into account all interparticle forces, is beyond the scope of this paper and will be presented elsewhere. Stability and oscillations can also be discussed in a simplified 1D model. We will show that undamped or even temporally growing, oscillating solutions for the upper and lower particles exist at a finite value of the damping constant.

This model consists of interacting chains of masses and springs (see Fig. 5). The repulsive forces between the upper and lower particles and the attractive force on the lower particle due to the positive charge are explicitly taken into account only for the three particles at each chain position. The repulsive forces of neighboring particles are represented by a spring k_1 for the upper and lower chains, which in principle could be adjusted for shielding. The additional attractive force on the particles of the lower layer by the positive charges of the neighboring chain positions leads to a different effective spring k_2 for the lower layer. It may be anticipated that $k_2<k_1$ because the attractive force weakens the repulsive force for the lower chain.

So we end up with the following set of equations:

$$\ddot{x}_1^{(n)}+\nu\dot{x}_1^{(n)}=\frac{k_1}{m}(x_1^{(n-1)}-2x_1^{(n)}+x_1^{(n+1)})+\frac{A}{d^3}(x_1^{(n)}-x_2^{(n)}), \tag{1}$$

$$\ddot{x}_2^{(n)}+\nu\dot{x}_2^{(n)}=\frac{k_2}{m}(x_2^{(n-1)}-2x_2^{(n)}+x_2^{(n+1)})-\frac{A}{d^3}(x_1^{(n)}-x_2^{(n)}) + \gamma\frac{A}{d_i^3}(x_1^{(n)}-x_2^{(n)}), \tag{2}$$

where $x_1^{(n)}, x_2^{(n)}$ are the horizontal displacements of the nth upper and lower particles, respectively, and $A=Z^2e^2/4\pi\epsilon_0 m$, where e is the elementary charge, ϵ_0 is the permittivity of free space, and m is the mass of the dust particles. The terms containing A are the linearized repulsive and attractive forces. ν is the damping constant due to friction with the neutral gas background [12]. The dots denote time derivatives. Shielding effects are here neglected for simplicity. With the usual ansatz for waves on linear chains $x_j^{(n)}=\exp(inqa)x_j$, where q is the wave number, Eqs. (1) and (2) have the solution

$$x_j=x_{j,0}\exp(\lambda t), \quad j=1,2$$

where

$$\lambda=-\frac{\nu}{2}\pm\sqrt{\frac{\nu^2}{4}-\omega_*^2}\pm\sqrt{C^2/4+K\left(K+\frac{\gamma}{\delta^3}\frac{A}{d^3}\right)}. \tag{3}$$

Here

$$\omega_*^2=2\frac{k_1}{m}(\kappa+1)\sin^2(qa/2)+\frac{C}{2},$$

$$C=A/d^3(\gamma/\delta^3-2),$$

$$K=2\frac{k_1}{m}(\kappa-1)\sin^2(qa/2),$$

and $\kappa=k_2/k_1$. This system describes three different types of solutions. For $\omega_*^2<0$ we have a nonoscillating unstable system for any value of ν. For $\omega_*^2>0$—a sufficient condition for this is $\gamma/\delta^3>2$, which means that the attractive force is larger than twice the repulsive force—one finds a critical value of the damping constant ν_*, above which the system is aligned and stable and below which it is oscillating with growing amplitude. Oscillations appear when the inner square root of (3) becomes imaginary at

$$\nu_*=\omega_*^{-1}\mathrm{Im}[\sqrt{C^2/4+K(K+\gamma A/\delta^3 d^3)}]. \tag{4}$$

A necessary but not sufficient condition is $K<0$, which means that the lower spring k_2 must be weaker than the upper k_1, and $K+\gamma A/\delta^3 d^3>0$. The latter condition can be fulfilled by the attractive force of the positive point charge. Here one clearly sees that the asymmetric forces are responsible for the existence of these undamped oscillations. If this asymmetry is absent, then the inner square root collapses to $\sqrt{C^2/4+K^2}$; therefore it will not be imaginary, and all oscillations will be damped.

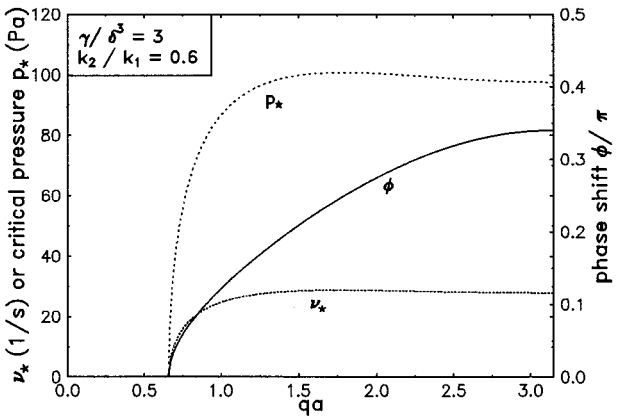

FIG. 6. Critical damping constant ν_*, corresponding pressure p_*, and phase shift as a function of the wave number.

Undamped oscillations of the dust particles in the presence of friction arise because of available free energy. In our model the source is the positive point charge which provides an attractive force on the lower particle without itself being attracted by the lower particle. In the real physical system the source of free energy is provided by the streaming ions, which create the ion cloud below the upper particle that attracts the lower particles.

In the simplified model there exists a range of values of γ/δ^3 and k_2/k_1, for which the critical damping constant attains nonzero values. The critical value of the damping constant ν_*, the amplitude ratio $|x_{2,0}/x_{1,0}|$, and the phase difference of the oscillations can now be calculated. For the amplitude ratio one finds the simple result $|x_{2,0}/x_{1,0}|=\sqrt{\gamma/\delta^3-1}$, independent of the wave number and κ. Hence for $\gamma/\delta^3>2$, the oscillation amplitude of the lower particle is larger than that of the upper. In Fig. 6, ν_*, the corresponding critical pressure p_*, [12] and the phase lead of the upper particle with respect to the lower are shown as a function of the wave number for $\gamma/\delta^3=3$ and $\kappa=0.6$. $k_1/m=2A/a^3$ is obtained from nearest-neighbor interaction only. For long wavelengths no temporally growing oscillations exist. Oscillations can occur below a value of 100 Pa for wave numbers about $qa=1.75$. The corresponding phase shift is about $\pi/4$. These values are comparable to the experimental values. Of course these results depend on the exact values of the parameters, but the critical pressure is always found between 30 and 200 Pa at small wavelength. It is found that the upper particle always has a phase lead between 0 and $\pi/2$, which agrees with the observations. It must be admitted that an uncertainty lies in the calculation of k_1, since only nearest neighbors are taken into account and screening is neglected. However, our simplified model is able to explain the oscillation mechanism with reasonable agreement with experiment.

In conclusion, we have shown that ion streaming around dust grains is responsible for the alignment of the crystal and for the onset of unstable oscillations. From a quantitative analysis under realistic conditions and taking collisions into account, the aligned structure is found to be energetically favored over the hcp structure. A simple 1D model is able to predict the sharp boundary between the stable alignment and the oscillations in the presence of frictional damping as observed in the experiment. The crucial idea behind the instability is the introduction of nonreciprocal forces that reflect the symmetry breaking by streaming ions. This instability can also be considered as the energy source that leads to the experimentally observed heating of the dust particles [8] during the melting transition.

This work was supported by the DFG (Pi185/8-1), INTAS (94-740), the Russian Foundation for Fundamental Investigation (94-02-03326), and Soros Foundation (SU N1600).

[1] H. Ikezi, Phys. Fluids **29**, 1764 (1986).
[2] J. H. Chu, J.-B. Du, and Lin I, J. Phys. D **27**, 296 (1994).
[3] J. H. Chu and Lin I, Physica A **205**, 183 (1994).
[4] J. H. Chu and Lin I, Phys. Rev. Lett. **72**, 4009 (1994).
[5] H. Thomas *et al.*, , Phys. Rev. Lett. **73**, 652 (1994).
[6] A. Melzer, T. Trottenberg, and A. Piel, Phys. Lett. A **191**, 301 (1994).
[7] T. Trottenberg, A. Melzer, and A. Piel, Plasma Sources Sci. Technol. **4**, 450 (1995).
[8] A. Melzer, A. Homann, and A. Piel, Phys. Rev. E **53**, 2757 (1996).
[9] S. V. Vladimirov and M. Nambu, Phys. Rev. E **52**, 2172 (1995).
[10] F. Melandsø and J. Goree, Phys. Rev. E **52**, 5312 (1995).
[11] T. J. Sommerer, W. N. G. Hitchon, R. E. P. Harvey, and J. E. Lawler, Phys. Rev. A **43**, 4452 (1991).
[12] P. S. Epstein, Phys. Rev. **23**, 710 (1924).